Theoretical Studies of Stability and Reactivity of C_2 Hydrocarbon Species on Pt Clusters, Pt(111), and Pt(211)

Ramchandra M. Watwe,[†] Randy D. Cortright,[†] Jens K. Nørskov,[‡] and James A. Dumesic*,[†]

Department of Chemical Engineering, University of Wisconsin, Madison, Wisconsin 53706, and Center for Atomic-scale Materials Physics, Technical University of Denmark, DK-2800 Lyngby, Denmark

Received: September 10, 1999; In Final Form: January 6, 2000

Quantum chemical calculations employing density functional theory were performed to investigate the interactions of C_2H_x(ads) species on Pt_{10} clusters and on Pt(111) and Pt(211) slabs. We calculate the binding energies of experimentally observed surface species, such as di-σ-bonded ethylene, ethylidyne species, and di-σ/π vinylidene species. In addition, we calculate the binding energies of the other species, such as ethyl, ethylidene, and vinyl species, that are postulated to be reactive intermediates in surface reactions. Furthermore, we calculate the activation energies for C−C bond dissociation of various C_2H_x(ads) species. We show that the bonding energies are dependent on the geometry of the surface, leading to the observed structure sensitivity of ethane hydrogenolysis. We show that the underlying parameter for understanding the stronger binding of various species on the step edge of Pt(211) compared to Pt(111) is the position of the metal d-band center. With estimates from these DFT calculations of the potential energy surface involved in the formation and reactivity of various C_2H_x(ads) species on Pt, we show that the primary reaction pathways for ethane hydrogenolysis on platinum involve highly hydrogenated species, such as C_2H_5(ads).

Introduction

In recent years, computational methods using density functional theory (DFT) have rapidly progressed owing to advances in computational speed, along with the development of new algorithms. For example, DFT methods have proven to be useful to predict accurate geometries and reasonable energetics for molecules containing transition metals.[1−5] The results of quantum chemical calculations, therefore, complement the results of experimental investigations of stable adsorbed species. Furthermore, these calculations can be used to predict the energetics of highly reactive intermediates and transition states that cannot be observed experimentally.[6] We show in the present paper the utility of quantum chemical, DFT techniques in obtaining structural and energetic parameters for simple hydrocarbon surface reactions, using metal clusters and two-dimensional slabs to describe the catalyst surface. In particular, we have investigated various adsorbed C_2H_x(ads) species on Pt surfaces, and we have identified the corresponding transition states for cleavage of the C−C bond in these adsorbed species.

We use the results from our DFT computational studies to address the factors controlling the rate of ethane hydrogenolysis over Pt catalysts. This reaction has been used as a probe of the catalytic properties for various supported metal and metal−alloy catalysts.[7] For example, the catalytic activity for ethane hydrogenolysis depends on the size of metal catalyst particles,[8] and various kinetic studies on single-crystal surfaces have shown that the reaction rate depends on the type of surface.[8] For a given metal, open planes show higher catalytic activity than the close-packed face.[8] To address the origin of this structure sensitivity for ethane hydrogenolysis, we have compared the energetics for the formation and reactivity of C_2H_x(ads) species on the (111) and (211) surfaces of Pt.

For comparison with our DFT computational results, we refer to a wide range of experimental studies that address the interactions of ethylene with single-crystal platinum surfaces[9−14] and with supported platinum catalysts.[15−17] The results of these investigations of ethylene adsorption on various Pt surfaces at different temperatures reveal the presence of distinct surface species, such as π-bonded ethylene, di-σ-bonded ethylene, and ethylidyne species. The strengths with which these species interact with Pt have been probed microcalorimetrically over platinum single crystals at 300 K,[18−20] over platinum powder and silica-supported Pt at 303 K,[15,21,22] and over platinum powder and silica-supported Pt at temperatures lower than 270 K.[15,23]

Methods

1. Cluster Approach. Density functional theory calculations for 10-atom Pt clusters were carried out with Jaguar software (Schrodinger, Inc.).[24] The chosen density functional uses a hybrid method employing Becke's three-parameter approach, B3LYP.[25] This functional combines the exact HF exchange, Slater's local exchange functional, and Becke's 1988 non-local gradient correction to the exchange functional with the correlation functionals of Vosko−Wilk−Nusair (VWN) and Lee−Yang−Parr (LYP).

The basis set employed in all calculations uses an effective core potential on all Pt atoms.[26] The electrons treated explicitly on Pt are the outermost core and valence electrons ($5s^2\ 5p^6\ 5d^9\ 6s^1$), with the remaining core electrons treated with effective core potentials. The C and H atoms have been treated with the 6-31G** basis set,[27] with all electrons being considered explicitly.

We have studied the interaction of various C_2H_x(ads) species with a constrained, 10-atom platinum cluster (Figure 1a), for which the Pt−Pt bond distances were fixed at the bulk value of 2.77 Å. The Pt_{10} cluster is comprised of three layers containing 6, 3, and 1 Pt atoms. These three layers correspond to (111) planes stacked in the ABC arrangement of the bulk fcc crystal

* To whom correspondence should be addressed.
[†] University of Wisconsin.
[‡] Technical University of Denmark.

10.1021/jp993202u CCC: $19.00
Published on Web 02/11/2000

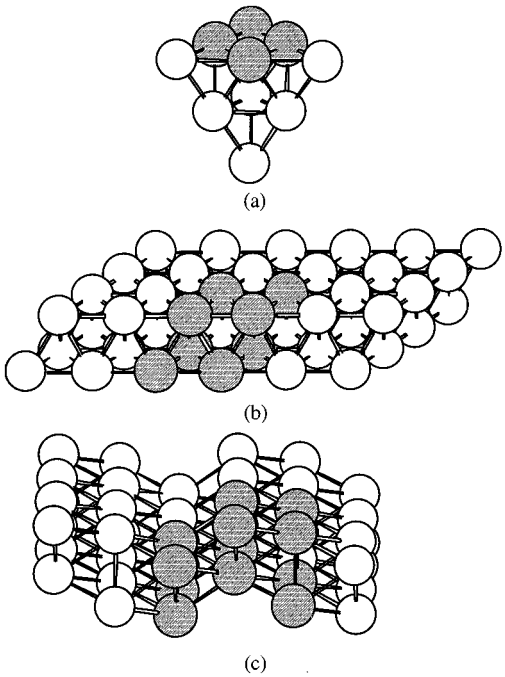

Figure 1. Models of platinum clusters and slabs: (a) Pt_{10} cluster; (b) Pt(111) slab; (c) Pt(211) slab. Shaded atoms in the cluster are used in optimizations of stable species and activated complexes. Shaded atoms in the slabs illustrate the super cell used for slab calculations.

structure. Location of transition states is a computationally difficult and expensive task. It is necessary to calculate the Hessian matrix to confirm the existence of one negative eigenvalue. To reduce the computational effort, we have used smaller metal clusters to locate the transition states for various reactions studied in this paper. Accordingly, only those platinum atoms which are directly bonded to the carbon atoms of the hydrocarbon species in the reactant or the transition state are used to locate the reactant and transition state geometries. For C−C bond scission of ethyl and di-σ-bonded ethylene species, we have used three platinum atoms, and for other species, namely, vinyl, ethylidene, and di-σ/π vinylidene species, we have used four platinum atoms in the location of transition state structures. The Pt−Pt distances were frozen at the bulk value of 2.77 Å during the transition state and reactant optimizations. The optimized small clusters were then embedded in 10-atom platinum clusters. Single-point energy calculations were conducted on these clusters to estimate heats of reactions to form activated complexes for the various C−C bond cleavage reactions.

We have corrected the electronic energy changes for various reactions to obtain enthalpy changes at higher temperatures by including the zero-point energies and thermal corrections. These corrections are obtained from the smaller clusters, and they are calculated from the vibrational frequencies of the adsorbed complexes. The entropies of the various surface species were also determined from the calculated frequencies.

2. Slab Approach. We have primarily used two-layer slabs of Pt(111) and Pt(211), periodically repeated in a super cell geometry with four equivalent layers of vacuum between any two successive metal slabs. These slabs are shown in parts b and c of Figure 1. We have also used three layer slabs to investigate the effect of the slab thickness on the calculated binding energies for several adsorbates. The calculated equilibrium lattice constant was 4.00 Å. A 2×2 unit cell was used to study the adsorption of various species, corresponding to $^1/_4$ monolayer coverage. Adsorption occurs on one side of the slab,

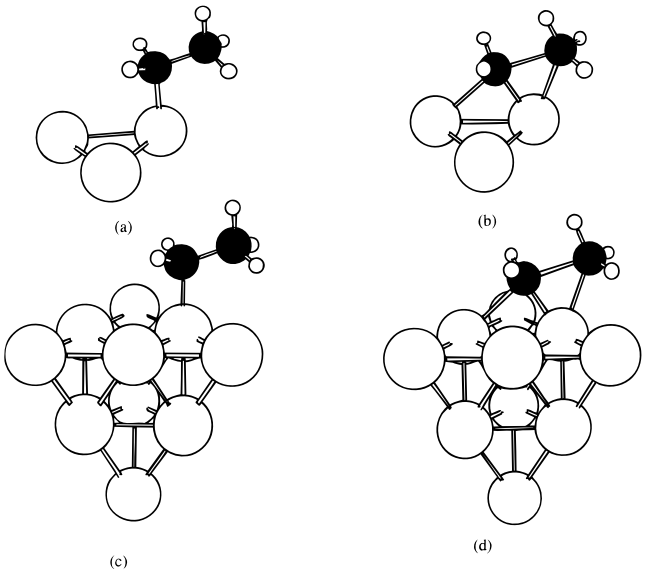

Figure 2. Adsorption of (a) ethyl species and (b) activated ethyl species on a three-atom platinum cluster and embedded in Pt_{10} clusters (c and d), respectively.

to avoid errors originating from the spurious interactions of adsorbates through the slab. In most calculations, the adsorbate atoms were allowed to relax, while the surface layer was kept fixed; however, we also investigated the effects of surface atom relaxations in several cases. Ionic cores are described by ultrasoft pseudopotentials,[28] and the Kohn−Sham one-electron valence states are expanded in a basis of plane waves with kinetic energies below 25 Ry. The surface Brillouin zone is sampled at 18 special k-points. The exchange-correlation energy and potential are described by the generalized gradient approximation (PW-91).[29,30] The self-consistent PW-91 density is determined by iterative diagonalization of the Kohn−Sham Hamiltonian, Fermi-population of the Kohn−Sham states ($k_BT = 0.1$ eV), and Pulay mixing of the resulting electronic density.[31] All the reported binding energies are calculated using the PW-91 functional, and these energies have been extrapolated to $k_BT = 0$ eV. We also report non-self-consistently determined chemisorption energies for a recently developed exchange-correlation energy functional called the RPBE functional.[32] We have used the nonspin polarized version of the exchange-correlation functional. We have tested the validity of this approximation by conducting a spin-polarized calculation for ethylidyne species on Pt(111), and we find that the electronic energy change of adsorption is identical to the value obtained from the nonspin polarized calculation.

Results

1. Pt_{10} Clusters. Figure 2a shows the optimized geometry of an ethyl group adsorbed on a three-atom platinum cluster, and Figure 2b also shows the corresponding transition state structure for the C−C bond scission of the ethyl group to form a methyl and methylene species. The plane passing through the C−C bond in the ethyl group and the Pt atom to which the ethyl group is bound was constrained to be perpendicular to the plane of the Pt_3 cluster. The reactant species and the transition state structure were then embedded in Pt_{10} clusters, as shown in parts c and d of Figure 2, and single-point energy calculations were carried out on both of these structures. The Pt−C and C−C bond lengths of all these species are summarized in Table 1. The energy changes to form stable species and the corresponding activated complexes are given in Tables 2 and 3, respectively.

TABLE 1: Bond Lengths (Å) in Stable Adsorbed Species and Transition States and Activation Energies (kJ/mol) for the Elementary Steps for C−C Bond Dissociation[a,b]

		bond lengths in stable species					bond lengths in transition states					
species	figures	Pt−C				C−C	Pt−C				C−C	E_{act}[c]
						Pt_{10}						
C_2H_5	2c,d	2.01				1.54	1.97	2.37	2.37		1.96	155
C_2H_4	3a,b	2.03	2.03			1.52	1.88	1.97	2.37		2.12	262
C_2H_4	3c,d	2.03	2.03			1.52	1.99	1.99	2.24	2.24	1.95	350
$CHCH_3$	4a,b	2.03	2.03			1.52	1.94	1.94	2.18	2.30	1.89	55
$CHCH_2$	4c,d	2.00	2.02	2.02		1.49	1.92	1.92	1.93		2.12	135
CCH_2	4e,f	1.89	1.89	2.02	2.15	1.42	1.88	1.88	2.04	2.08	2.06	211
						Pt(111)						
C_2H_5	5d, 7a	2.13				1.51	2.08	2.12	2.25		2.08	173
$CHCH_3$	5e, 7b	2.08	2.08			1.50	2.00	2.00	2.17	2.33	1.99	106
$CHCH_2$	5f, 7c	2.08	2.10	2.10		1.47	1.97	1.97	2.21	2.34	2.21	160
						Pt(211)						
C_2H_5	6a, 8a	2.10				1.50	2.06	2.10	2.22		2.08	102
C_2H_4	6b, 8b	2.12	2.12			1.48	1.95	2.02	2.37		2.21	193
$CHCH_3$	6c, 8c	2.05	2.05			1.50	1.99	2.01	2.14	2.30	1.99	163
$CHCH_2$	6e, 8e	2.07	2.09	2.09		1.47	1.94	1.94	1.99		2.21	161
$CHCH_2$	6f, 8f	2.05	2.06	2.49		1.48	1.93	1.95	2.11	2.27	2.17	87

[a] The results for Pt(111) and Pt(211) are obtained from the PW-91 functional. The use of the RPBE functional results in the activation energies being higher by 9 ± 6 kJ/mol. [b] The H−C−H and C−C−H angles in the stable hydrocarbon species are 109° ± 2° and 112° ± 2°. For comparison, the normal H−C−H and C−C−H angles in C_2H_6 are 108° and 111°, respectively. [c] E_{act} corresponds to the energy change from the stable C_2H_x adsorbed species to form the corresponding activated complex for cleavage of the C−C bond.

TABLE 2: Electronic Energy Changes for Reactions Involving the Formation of Stable Species Adsorbed on Platinum (kJ/mol)[a]

reaction	Pt_{10}	Pt(111)	Pt(211)
$Pt + C_2H_6 \rightarrow PtC_2H_5 + 0.5H_2$	28	51	6
$Pt + C_2H_6 \rightarrow PtC_2H_4$ (di-σ) $+ H_2$	68	70	−1
$Pt + C_2H_6 \rightarrow PtCHCH_3 + H_2$	107	104	19
$Pt + C_2H_6 \rightarrow PtCCH_3 + 1.5H_2$	13	58	45
$Pt + C_2H_6 \rightarrow PtCHCH_2 + 1.5H_2$	121	128	80
$Pt + C_2H_6 \rightarrow PtCCH_2 + 2H_2$	149	157	138
$2Pt + H_2 \rightarrow 2PtH$		−85	−146
$C_2H_6 \rightarrow C_2H_4 + H_2$	170	171	171
$C_2H_6 \rightarrow C_2H_2 + 2H_2$	400	393	393

[a] The results for Pt(111) and Pt(211) are obtained from the PW-91 functional. The use of the RPBE functional results in the energies being more endothermic by 32 ± 5 kJ/mol.

TABLE 3: Electronic Energy Changes for Reactions Involving the Formation of Activated Complexes Adsorbed on Platinum (kJ/mol)[a]

reaction	Pt_{10}	Pt(111)	Pt(211)
$Pt + C_2H_6 \rightarrow PtC_2H_5^{\ddagger} + 0.5H_2$	183	224	108
$Pt + C_2H_6 \rightarrow PtC_2H_4^{\ddagger}$ (di-σ) $+ H_2$	330		192
$Pt + C_2H_6 \rightarrow PtCHCH_3^{\ddagger} + H_2$	162	210	182
$Pt + C_2H_6 \rightarrow PtCHCH_2^{\ddagger} + 1.5H_2$	256	288	241
$Pt + C_2H_6 \rightarrow PtCCH_2^{\ddagger} + 2H_2$	360		

[a] The results for Pt(111) and Pt(211) are obtained from the PW-91 functional. The use of the RPBE functional results in the energies being more endothermic by 44 ± 7 kJ/mol.

We have examined two modes of C−C bond breaking of di-σ-adsorbed ethylene species. Figure 3a shows di-σ-adsorbed ethylene on the edge of the platinum cluster. The C−C bond in this species is activated in a sliding motion to form the transition state structure shown in Figure 3b. Another mode of C−C bond activation is shown in parts c and d of Figure 3, involving cleavage of the C−C bond over a 3-fold site of the platinum cluster.

Figure 4a shows the adsorbed ethylidene species, $CHCH_3$-(ads), on the platinum cluster. The corresponding transition state structure for C−C bond activation to form CH(ads) and CH_3(ads) surface species is shown in Figure 4b. The activation energy for this elementary step was calculated to be 55 kJ/mol,

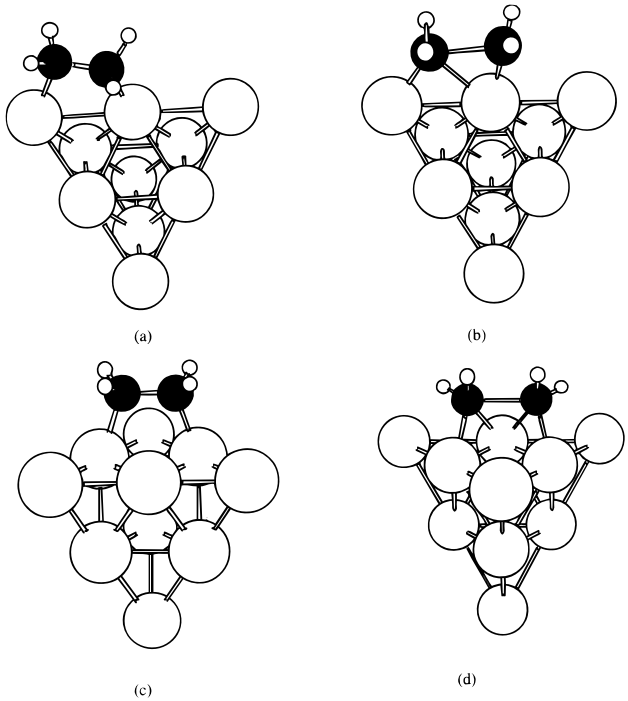

Figure 3. Adsorption of di-σ-bonded ethylene in two different configurations (a and c) and corresponding activated complexes (b and d).

the lowest among those examined in this paper. Parts c and e of Figure 4 show vinyl species and di-σ/π vinylidene species on the platinum cluster, and parts d and f show the corresponding activated complexes. We note that we have used corner atoms of Pt_{10} cluster to calculate the activated di-σ ethylene and di-σ/π vinylidene species because of the small size of the Pt_{10} cluster.

2. Adsorption of Hydrogen on Pt(111) and Pt(211). Hydrogen atoms adsorb on 3-fold sites on the Pt(111) surface. The calculated energies for dissociative adsorption of a dihydrogen molecule for 1/4 monolayer and full monolayer coverages are −85 and −81 kJ/mol, respectively. Hence, there appears to be minimal adsorbate−adsorbate interactions between hydrogen atoms on Pt(111). There is a large variation in the

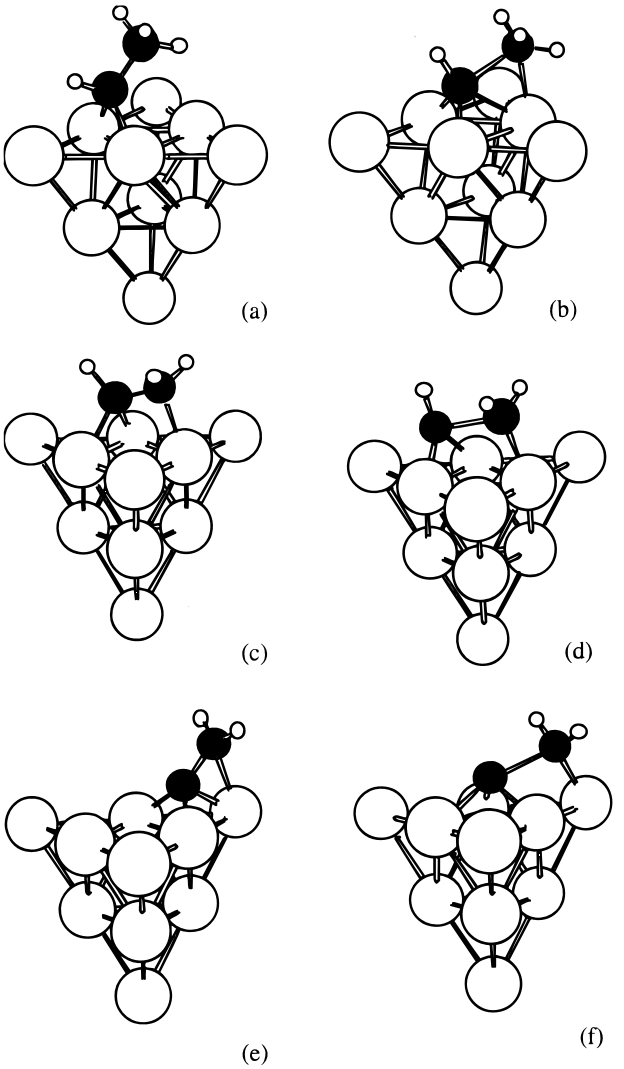

Figure 4. Adsorption of (a) ethylidene species, (b) activated ethylidene species, (c) vinyl species, (d) activated vinyl species, (e) di-σ/π vinylidene species, and (f) activated di-σ/π vinylidene species on Pt_{10} cluster.

reported heats of hydrogen adsorption on platinum with values ranging from −40 to −105 kJ/mol (see, for example, ref 33). The experimental value for the heat of H_2 dissociation is equal to −90 kJ/mol for supported platinum catalysts and platinum powder.[23,34] The Pt−H bond length is calculated to be 1.87 Å, and this value is between the experimental values of 1.76 and 1.90 Å that have been reported for the Pt−H bond length.[35] Hydrogen adsorbs on a 2-fold site on the step edge of Pt(211). The energy of dissociative adsorption of a dihydrogen molecule is calculated to be −146 kJ/mol. The Pt−H bond length is 1.75 Å. The calculated values for the energetics of various species adsorbed on Pt(111) and Pt(211) are summarized in Table 2.

3. Adsorption of Ethylene on Pt(111). Various theoretical studies have addressed the adsorption of ethylene on platinum.[5,6,36−39] We have investigated di-σ-bonded ethylene having the traditional symmetrical structure with the C−C axis oriented parallel to the Pt surface, and we have considered a recently proposed asymmetrical structure with the C−C axis tilted slightly with respect to the Pt surface plane. The optimized geometries of these two structures are shown in parts a and b of Figure 5, respectively. We find that the binding energies of ethylene in the symmetrical and asymmetrical modes are −101 and −38 kJ/mol, respectively. Hence, our calculations predict that the traditional structure of di-σ-bonded ethylene, where the tetravalency of carbon is preserved, is more stable on Pt(111), in contrast to a LEED study.[40] This result is in agreement with recent DFT calculations of ethylene chemisorption on Pt(111), which show the binding energies of ethylene in symmetrical and aysmmetrical modes to be −107 and −62 kJ/mol.[39]

King and co-workers have reported that the heat of ethylene adsorption to form di-σ-bonded ethylene is equal to −136 kJ/mol on a Pt(110)(2 × 1) surface at room temperature.[18] Microcalorimetric results from our group for ethylene adsorption on platinum powders at 173 K show a heat of −120 kJ/mol,[23] conditions for which di-σ-bonded ethylene species are predominant on the surface.[15] Our calculations indicate that the Pt−C and C−H bond lengths in the symmetrical mode are 2.13 and 1.10 Å, respectively. The H−C−H, C−C−H, and Pt−C−H angles are 112°, 114°, and 103°, respectively. The C−C bond length is calculated to be 1.48 Å, and this value is in good agreement with experimental values of 1.48−1.52 Å.[41,42] The calculated value of the C−C bond length is close to the C−C bond length in ethane (1.54 Å) and is considerably longer than that in ethylene (1.34 Å), indicating rehybridization of the C−C bond from sp^2 to sp^3. This rehybridization has been seen experimentally on Pt(111) at low temperatures.[16,17] The asymmetrical mode of di-σ-bonded ethylene adsorbs on a 3-fold site, with the three Pt−C bond lengths being equal to 2.21, 2.27, and 2.27 Å, and the C−C bond length equal to 1.47 Å. The tilt of C−C axis with respect to the surface plane is 11°. These structural parameters are in agreement with LEED measurements.[40]

Studies of the interactions of ethylene with Pt(111) at temperatures above 280 K indicate that ethylene adsorbs dissociatively and rearranges such that the C−C axis is oriented perpendicular to the surface.[17] The resulting ethylidyne species prefers the 3-fold, fcc site on Pt(111), as shown in Figure 5c. Our DFT calculations for adsorbed ethylidyne species at 3-fold hollow sites give a C−C bond length of 1.48 Å and Pt−C bond lengths of 2.02 Å. The hydrogen atoms point toward the bridge positions on Pt(111). This geometry agrees with results from LEED studies reported by Somorjai and co-workers, which indicate a C−C bond length of 1.50 ± 0.05 Å and Pt−C bond lengths of 2.00 ± 0.05 Å.[14] The energy change for the formation of ethylidyne species from gas-phase ethylene with the liberation of gas-phase dihydrogen is −113 kJ/mol. Since the energy of H_2 adsorption on Pt(111) is calculated to be −85 kJ/mol, the energy change for ethylene adsorption with the formation of ethylidyne species and hydrogen on the surface is −156 kJ/mol. King and co-workers reported a heat of −174 kJ/mol for adsorption of ethylene on Pt(111), which was attributed to the formation of ethylidyne species and coadsorbed H atoms.[19] Our group has reported a heat of −160 kJ/mol for ethylene interaction with Pt powder at 303 K.[23]

To study the effect of slab thickness and adsorption-induced surface relaxation, we have studied ethylidyne species on a three-layer Pt(111) slab, for which the upper layer of the slab was allowed to relax. The three platinum atoms bonded to ethylidyne species move upward by 0.09 Å, while there is a lateral expansion of the Pt−Pt bonds between these three Pt atoms by 0.04 Å, compared to the bulk value. Somorjai and co-workers have used LEED to observe a local expansion of 0.08 Å for the distance between the top two Pt layers upon formation of ethylidyne species, which is in agreement with our calculations.[43] On the other hand, these LEED studies showed that the three platinum atoms forming bonds to ethylidyne move closer to each other by 0.11 Å, while our calculations show otherwise. The C−C and Pt−C bond lengths

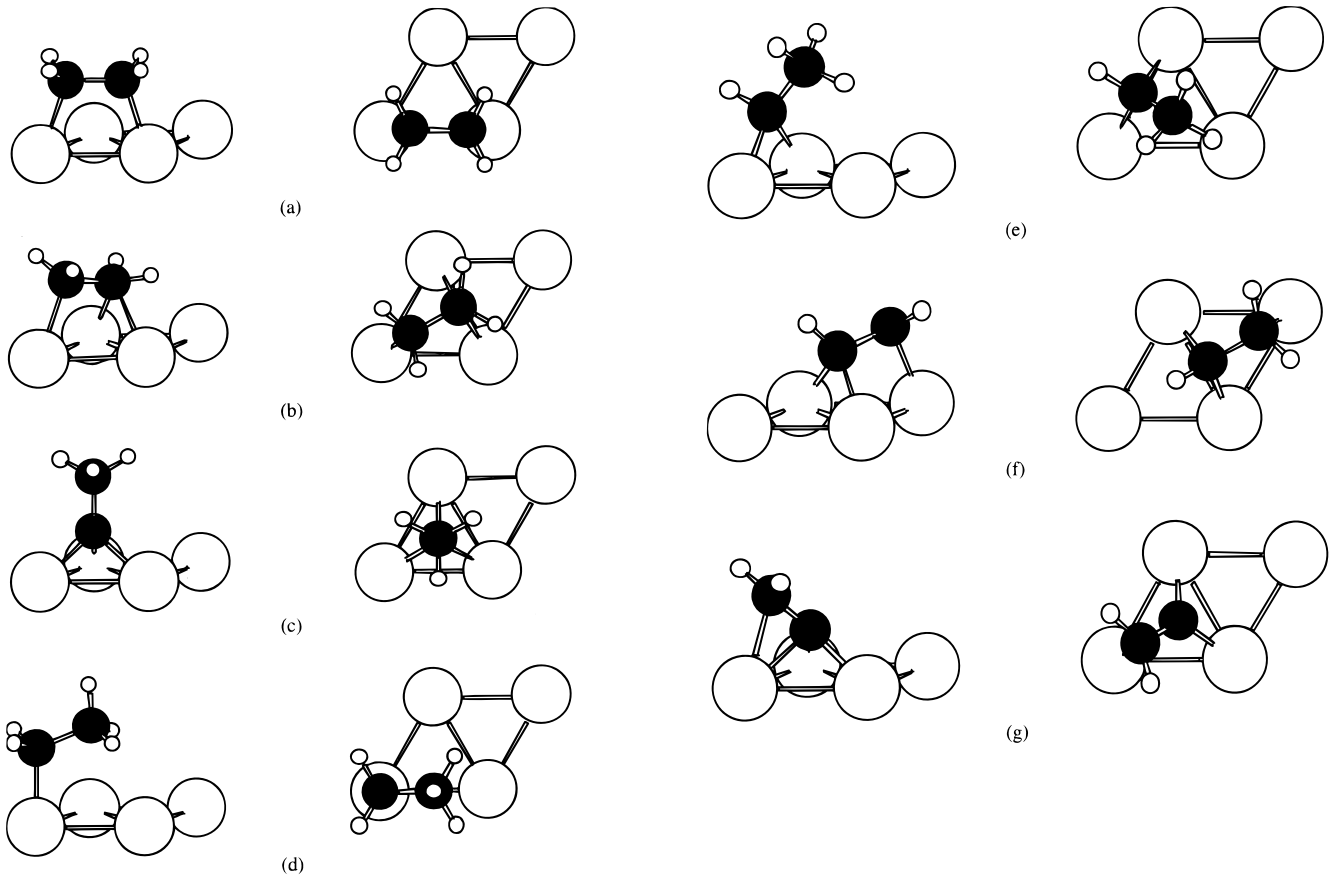

Figure 5. Side and top views of adsorption of di-σ-bonded ethylene on (a) bridge site and (b) 3-fold site, (c) ethylidyne species, (d) ethyl species, (e) ethylidene species, (f) vinyl species, and (g) di-σ/π vinylidene species on Pt(111).

for the ethylidyne species on the three-layer slab are 1.49 and 2.02 Å, respectively. The energy change for the formation of ethylidyne species from gas-phase ethylene with the liberation of gas-phase dihydrogen is −97 kJ/mol, which is more endothermic by 16 kJ/mol than the value predicted from the two-layer, fixed slab.

4. Adsorption of Ethylene on Pt(211). Figure 6b shows the optimized geometry of di-σ-bonded ethylene adsorbed on the step edge of Pt(211) surface. The step edge platinum atoms have a coordination number of 7, while the terrace platinum atoms have a coordination number of 9. The calculated binding energy of ethylene on Pt(211) is −172 kJ/mol, which is stronger than the binding of ethylene on Pt(111) by 71 kJ/mol. Figure 6d shows the optimized geometry of adsorbed ethylidyne species on the Pt(211) surface. The energy change for the formation of ethylidyne species on Pt(211) from gas-phase ethylene with the liberation of gas-phase dihydrogen is −126 kJ/mol, which is more exothermic than on Pt(111) by only 13 kJ/mol.

5. Hydrocarbon Fragments on Pt(111). Parts d−f of Figure 5 show the optimized geometries of C_2H_5(ads), $CHCH_3$(ads), and $CHCH_2$(ads) species on Pt(111). It appears that carbon binds at sites that preserve the tetrahedral geometry and saturate the coordination of the carbon atoms in these C_2H_x(ads) species. Ethyl species adsorbs on an atop site, with Pt−C and C−C bond lengths equal to 2.13 and 1.51 Å, respectively. The energy change for dissociative adsorption of ethane to form adsorbed ethyl species (Figure 5d) and gas-phase dihydrogen is 51 kJ/mol (endothermic). We have also investigated the adsorption of ethyl species on three-layer slabs with upper layer at bulk distance and upper layer relaxed. The corresponding energy changes are 47 and 40 kJ/mol. Hence, the energy changes caused by increasing slab thickness and surface atoms relaxation are small. The Pt−C and C−C bond lengths for ethyl species on the three-layer slab are 2.07 and 1.51 Å, respectively. The platinum atom bonded to ethyl species moves upward by 0.1 Å.

The adsorption of ethylidene species ($CHCH_3$(ads), see Figure 5e) prefers a 2-fold site on Pt(111). The Pt−C and C−C bond lengths are 2.08 and 1.50 Å. The energy change to form ethylidene species from gas-phase ethane with the liberation of gas-phase dihydrogen is 104 kJ/mol. The corresponding energy change is 92 kJ/mol on a relaxed, three-layer slab, and the Pt−C and C−C bond lengths are equal to 2.06 and 1.49 Å, respectively. The platinum atoms bonded to ethylidene species move up by 0.12 Å and the Pt−Pt bond length between these two platinum atoms contracts by 0.04 Å.

At temperatures higher than 280 K, acetylene has been shown to adsorb with the C−C axis tilted away from the platinum surface. We have shown in a previous study that this CCH_2(ads) species, denoted as di-σ/π vinylidene, is the most stable form of C_2H_2, on the platinum surface.[6] Figure 5g shows the optimized geometry of a CCH_2(ads) species with its C−C axis aligned at an angle of 43° to the surface. NMR studies of acetylene adsorption on small metal particles at room temperature have shown the existence of this species and the C−C bond length was determined to be 1.44 Å,[44] which is in agreement with our calculated value of 1.41 Å. The Pt−C bond lengths involved in σ-bonding are 1.98 Å. The calculated binding energy of acetylene to form this species is −236 kJ/mol.

6. Hydrocarbon Fragments on Pt(211). The optimized geometries of C_2H_5(ads), $CHCH_3$(ads), and $CHCH_2$(ads) species on Pt(211) are shown in parts a, c, and e of Figure 6. The Pt−C bonds involved in these adsorbed C_2H_x(ads) species are shorter on Pt(211) than on Pt(111) by 0.03, 0.03, and 0.01 Å,

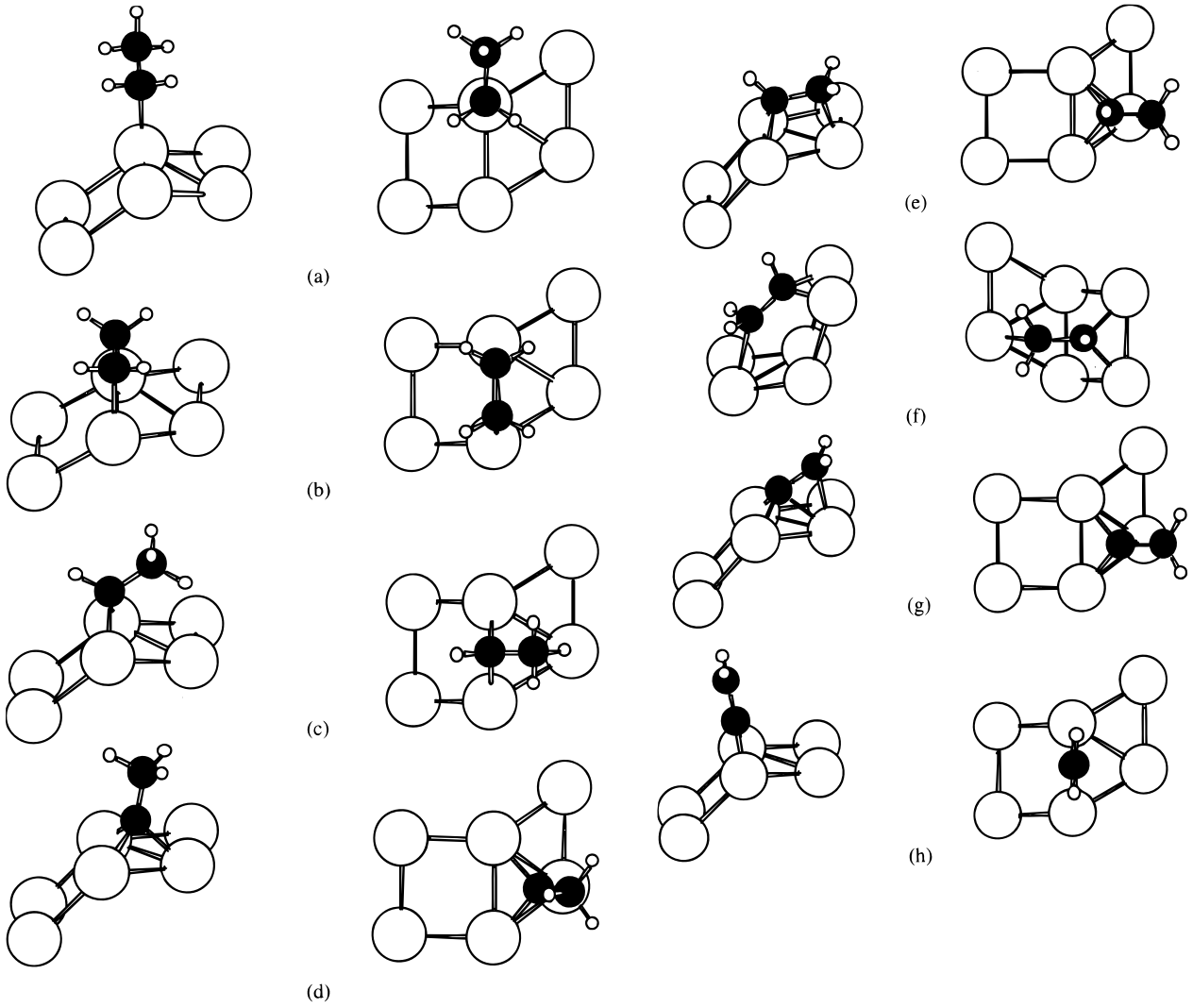

Figure 6. Side and top views of adsorption of (a) ethyl species, (b) di-σ-bonded ethylene, (c) ethylidene species, (d) ethylidyne species, (e) vinyl species on step edge, (f) vinyl species on the special site, (g) di-σ/π vinylidene species, and (h) μ_2-vinylidene species on Pt(211).

respectively. These species bind more strongly on Pt(211) than on Pt(111) by 45, 85, and 48 kJ/mol, respectively. We have also studied the adsorption of ethyl species on a three-layer Pt(211) slab, with the upper Pt layer free to relax. The calculated energy change for the formation of ethyl species on the surface from gas-phase ethane with the liberation of gas-phase dihydrogen is 7 kJ/mol, which is similar to the corresponding energy change of 6 kJ/mol over the two-layer Pt(211) slab. The platinum atom bonded to the ethyl species moves upward by 0.01 Å, while the neighboring platinum atom on the step edge moves downward by 0.17 Å, as a result of surface relaxation.

We have investigated a different form of $CHCH_2$(ads) species adsorbed on the step, as shown in Figure 6f. This species is bonded to Pt atoms on a step edge as well as on a different (111) terrace. This species is less stable than the $CHCH_2$(ads) species of Figure 6e by 92 kJ/mol. While one C atom in this species forms two bonds with the step edge, having bond length of 2.05 Å, the other C atom near the (111) terrace is at a longer distance of 2.49 Å from a Pt atom. The rationale behind studying such a species is to investigate the effect of the special geometry available at the step edge for C−C bond dissociation.

Figure 6g shows the di-σ/π vinylidene species adsorbed on the step edge of Pt(211). The C−C bond length is 1.41 Å and the Pt−C bond lengths involved in σ-bonding are 1.98 Å. The calculated energy of acetylene adsorption to form this species is −254 kJ/mol. This value is in agreement with a recent microcalorimetric study of acetylene on Pt(211) where the initial heat of adsorption is measured as -270 ± 10 kJ/mol, caused by the formation of vinylidene species on the step edge sites.[45] Figure 6h shows the μ_2-vinylidene species on Pt(211), for which the C−C bond length is 1.34 Å, corresponding to a C−C double bond. The energy of acetylene adsorption to form this species is −237 kJ/mol. Hence, the di-σ/π form of vinylidene species is slightly more stable than the μ_2-form of vinylidene species on the Pt(211).

7. C−C bond Activation on Pt(111) and Pt(211). We have conducted constrained geometry optimizations to map the potential energy surface for cleavage of the C−C bond for C_2H_5(ads), $CHCH_3$(ads), and $CHCH_2$(ads) species. In particular, we fix the value of the C−C bond length at various values and optimize the adsorbate on the Pt(111) and Pt(211) surfaces. After a series of such calculations, we locate an approximate maximum in the plot of energy versus C−C bond length. We also monitor the forces on the C atoms for the various intermediate structures in this plot, and we verify that the slope of these forces changes its sign at the energy maximum, verifying that the structure at this maximum is close to a transition state connecting the desired reactants and products.

Parts a−c of Figure 7 show approximate transition state structures for C−C bond dissociation of ethyl, ethylidene, and

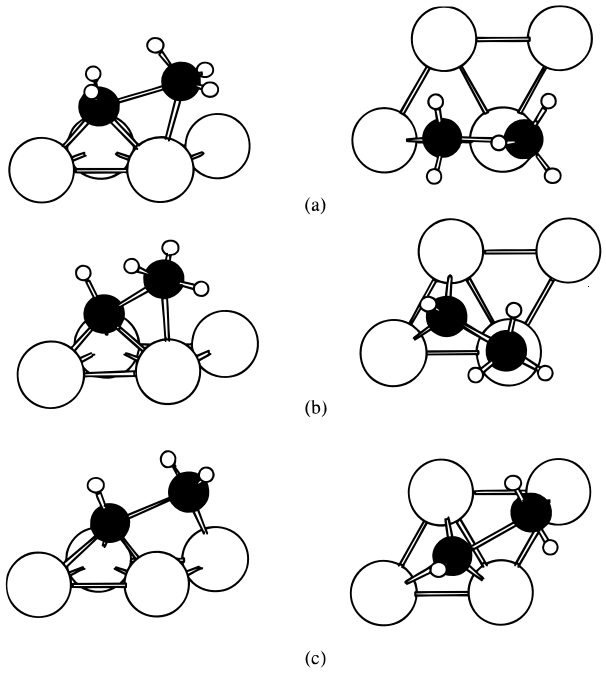

Figure 7. Side and top views of adsorption of activated (a) ethyl species, (b) ethylidene species, and (c) vinyl species on Pt(111).

vinyl species, respectively, on Pt(111). The Pt−C and C−C bond lengths involved in these species are given in Table 1. The approximate transition state structures for C−C bond dissociation of ethyl, di-σ-bonded ethylene, ethylidene, and vinyl species on Pt(211) surface are shown in Figure 8. The corresponding bond lengths are given in Table 1. We note that we have identified two transition states for C−C cleavage of ethylidene species ($CHCH_3$(ads), parts c and d of Figure 8), as well as two transition states for C−C cleavage of vinyl species ($CHCH_2$(ads), parts e and f of Figure 8). The configuration of the ethylidene activated complex shown in Figure 8c is more stable than the configuration shown in Figure 8d by 10 kJ/mol, since the former species makes more bonds with the step edge atoms. The configuration of the vinyl-activated complex shown in Figure 8e is more stable than the configuration shown in Figure 8f by 17 kJ/mol. The electronic energy changes for the formation of activated complexes from the corresponding stable species for the slab approach are given in Table 3.

We have also studied the activated complexes for C−C bond cleavage of adsorbed ethyl and ethylidene species on relaxed, three-layer slabs. The calculated energy change to form the ethyl activated complex from gas-phase ethane with the liberation of gas-phase dihydrogen on a relaxed, three-layer Pt(111) slab is 208 kJ/mol, compared to a value of 224 kJ/mol on a two-layer slab. The calculated energy change to form the ethylidene activated complex from gas-phase ethane with the liberation of gas-phase dihydrogen on a relaxed three-layer Pt(111) slab is 211 kJ/mol, compared to a value of 210 kJ/mol on a two-layer slab.

8. Enthalpies and Entropies of Surface Species. We have calculated vibrational frequencies of various C_2H_x(ads) species on the Pt_3 and Pt_4 clusters used in the constrained geometry optimizations involved in our studies of adsorption on 10-atom Pt clusters. We have used these frequencies to estimate zero-point energies and the thermal corrections to the electronic energies, and also to calculate the entropies of the surface species at 298 and 623 K. For a hydrocarbon species with n atoms (e.g., $n = 7$ for C_2H_5), we use $3n$ modes of vibration for stable reactive intermediates, and we use $3n - 1$ modes for transition states.

TABLE 4: Calculated Standard Entropies (at 1 atm), Zero-Point Energies, and Temperature Corrections to Enthalpies for Ethane, Dihydrogen, Stable Adsorbed Species, and Activated Complexes for C−C Bond Dissociation on Small Pt Clusters

species	entropies (J/mol/K)		ZPE (kJ/mol)	enthalpy corrections (kJ/mol)	
temperature (K)	298	623		298	623
C_2H_6 (gas phase)	228	278	197	12	35
C_2H_4 (gas phase)	219	260	134	10	29
C_2H_2 (gas phase)	202	240	70	10	27
H_2 (gas phase)	130	152	27	9	18
$[C_2H_5Pt_3]$	55	110	170	9	34
$[C_2H_4Pt_3]$	34	83	142	6	28
$[CHCH_3Pt_3]$	42	93	129	7	31
$[CCH_3Pt_3]$	40	85	109	7	27
$[CHCH_2Pt_4]$	24	68	109	5	25
$[CCH_2Pt_3]$	22	60	82	4	22
$[C_2H_5Pt_3]^‡$	44	95	168	7	31
$[C_2H_4Pt_3]^‡$	38	85	136	6	28
$[CHCH_3Pt_3]^‡$	36	83	137	6	28
$[CHCH_2Pt_4]^‡$	26	67	106	5	23

TABLE 5: Enthalpy and Standard (at 1 atm) Gibbs Free Energy Changes (kJ/mol) for Reactions Involving the Formation of Activated Complexes at 623 K

reaction	ΔH		$\Delta G°$	
	Pt(111)	Pt(211)	Pt(111)	Pt(211)
$Pt + C_2H_6 \rightarrow PtC_2H_5^‡ + 0.5H_2$	213	97	280	164
$Pt + C_2H_6 \rightarrow PtC_2H_4^‡ + 0.5H_2$		168		193
$Pt + C_2H_6 \rightarrow PtCHCH_3^‡ + H_2$	187	159	214	186
$Pt + C_2H_6 \rightarrow PtCHCH_2^‡ + 1.5H_2$	253	206	242	196

Table 4 presents a summary of these results for adsorbed ethyl, di-σ-bonded ethylene, ethylidene, and vinyl species, as well as for the activated complexes involved in C−C bond cleavage of these species. These corrections can be used to estimate the Gibbs free energy changes and enthalpy changes to form the activated complexes from gas-phase ethane with the liberation of gas-phase dihydrogen, as shown in Table 5. We note that these corrections are more important for reactions where several bonds are broken and formed. For example, the enthalpy change to form the activated di-σ-bonded ethylene on Pt(211) from gas-phase ethylene is lowered by only 1 kJ/mol when we include the thermal and zero-point energy corrections. On the other hand, the enthalpy change to form the activated di-σ-bonded ethylene on Pt(211) from gas-phase ethane with liberation of gas-phase dihydrogen is lowered by 24 kJ/mol when we include the thermal and zero-point energy corrections.

Discussion

Table 1 summarizes the lengths of the Pt−C and C−C bonds that are formed and broken during the formation of transition states from various C_2H_x(ads) species on Pt_{10} clusters, Pt(111) slabs, and Pt(211) slabs. This table shows that there are small differences in the predicted transition state structures between the cluster and slab approaches. The C−C bond lengths in the activated complexes are generally predicted to be longer in the slab approach compared to the cluster approach. This lengthening may be partially caused by the larger lattice constant used for slabs (4.00 Å) compared to clusters (3.92 Å).

We note that the RPBE functional predicts consistently lower binding energies than the PW-91 functional. In particular, the RPBE functional underpredicts the binding energies of the stable and activated species by 32 and 44 kJ/mol, respectively. However, we note that the difference is mainly caused by the change in the energy of species relative to the gas-phase ethane. Hence, the relative energies of different surface species are less sensitive to the choice of the functional. In particular, the RPBE

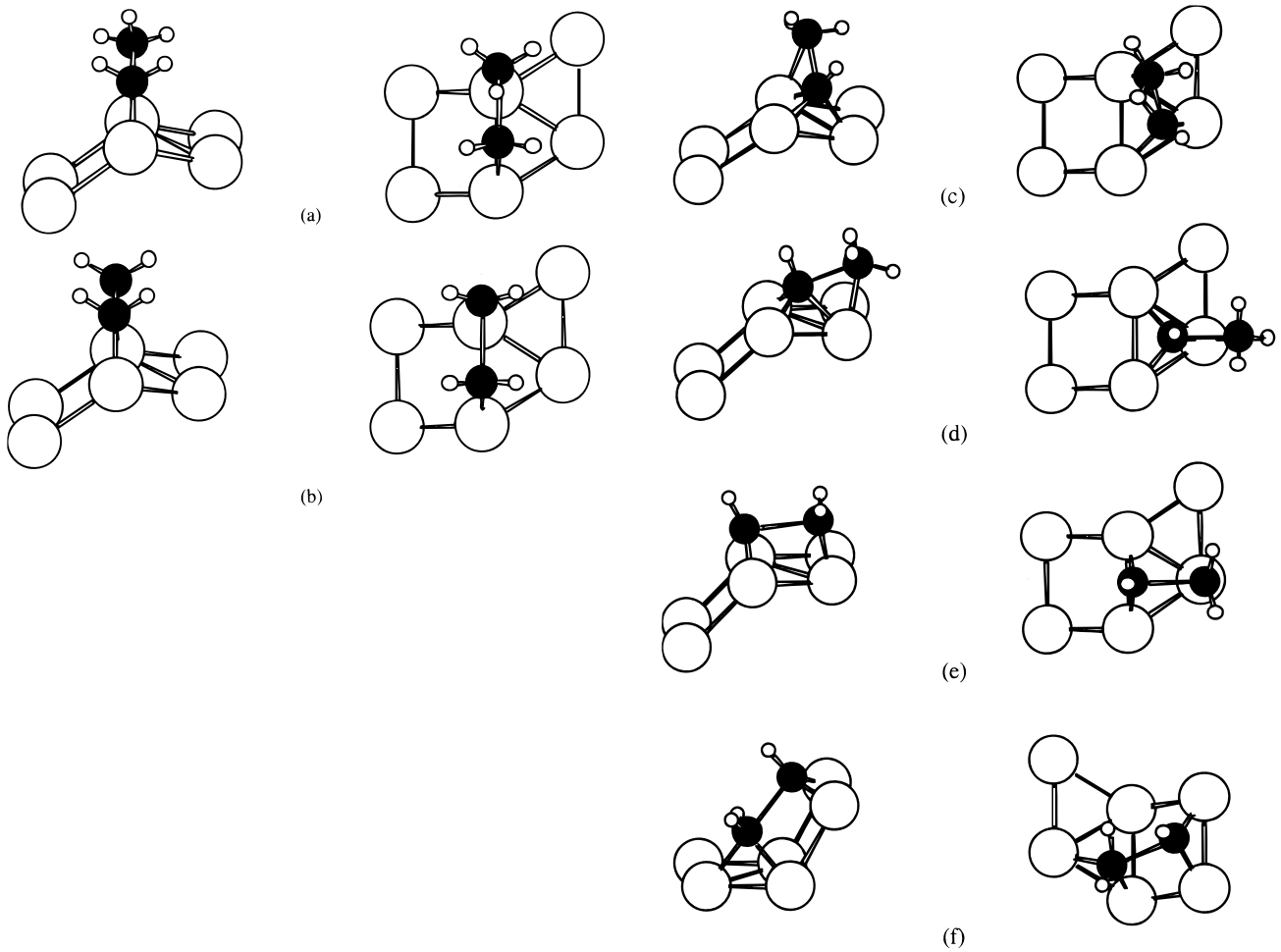

Figure 8. Side and top views of adsorption of activated (a) ethyl species, (b) di-σ-bonded ethylene, (c and d) ethylidene species, (e) vinyl species on the step edge, and (f) vinyl species on the special site of Pt(211).

functional predicts values for the activation barriers of the elementary steps that are higher by about 9 kJ/mol compared to the PW-91 functional.

Table 2 shows the electronic energy changes for the formation of stable species adsorbed on platinum with reference to gas-phase ethane and dihydrogen. We note that the energetics predicted using Pt_{10} clusters are comparable with those predicted for the Pt(111) surface, with the exception of the ethylidyne species. This similarity can be attributed to the fact that the Pt_{10} cluster can be viewed as three layers of (111) surfaces. Figure 9 shows a comparison between the electronic energies predicted by Pt_{10} clusters and Pt(111) slabs. We further note that the functionals used in the two approaches are not exactly the same and hence some variations may be expected in the calculated energetics.

We have recently reported results from DFT studies of stable C_2H_x(ads) species on fully optimized Pt_{10} clusters.[6] We note that in the former study we have optimized the hydrocarbon species as well as the Pt−Pt bond lengths for the Pt_{10} cluster, whereas in the present study we have optimized the hydrocarbon species on smaller Pt clusters and embedded these small clusters in constrained Pt_{10} clusters. In general, the fully optimized clusters give stronger binding of the hydrocarbon species than the constrained clusters.

While the energetics predicted from the cluster approach may depend on the cluster size and shape, the predicted structures of the adsorbates appear to be in good agreement with the available experimental data and with the more rigorous slab approach. This agreement makes the cluster approach a good

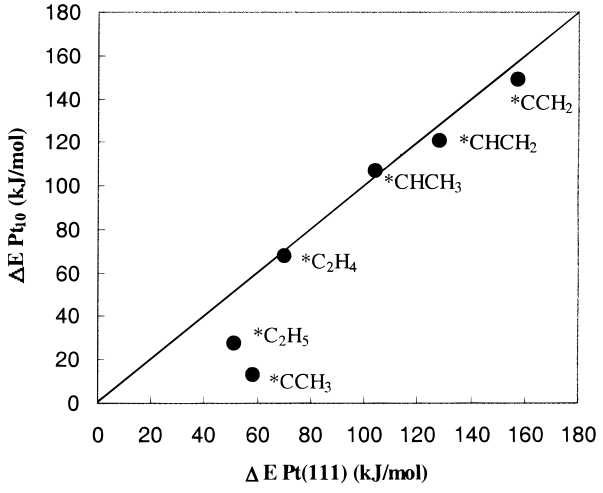

Figure 9. Comparison of binding energies (kJ/mol) obtained from Pt_{10} clusters versus Pt(111) slabs. Line shows points of equivalence between axes.

first approximation for more detailed studies using slabs. An advantage of the cluster approach is the ease of calculation of vibrational frequencies and hence the location of rigorous transition states. Therefore, we have used the cluster approach to obtain the vibrational frequencies needed to estimate entropies of the surface species, as well as the thermal corrections to the calculated electronic energy changes. These corrections play an important role when comparing the results from theoretical

TABLE 6: Pt−C Bond Energies (kJ/mol) for Pt(111) and Pt(211) Surfaces Calculated Using Average Bond Energy (abe) Method[a] and Valence Bond (vb) Method[b]

	Pt(111)		Pt(211)	
species	abe	vb	abe	vb
C_2H_5	154	156	199	200
C_2H_4	170	213	206	249
$CHCH_3$	153	170	196	213
CCH_3	186	228	190	232
$CHCH_2$	162	194	178	210
average	165	192	194	221

[a] Based on the average bond strengths for gaseous species (e.g., the reference state for gaseous CCH_3 used in these calculations is obtained by removing 3 H atoms from ethane, using an average value of 423 kJ/mol for each C−H bond). [b] Based on DFT calculations for gaseous species having the same electronic states as the adsorbed species (e.g., the reference state for gaseous CCH_3 used in these calculations is obtained from a DFT calculation of CCH_3 with a multiplicity of 4).

predictions with experimental data obtained at high temperatures, especially when several bonds are broken and formed during a reaction.

Metal−carbon bond strength is a fundamental quantity that can be used in the studies of surface reactions. Table 6 shows the calculated Pt−C bond strengths using an average bond energy (abe) method. For example, the electronic energy change to form surface ethylidyne species and gas-phase hydrogen atoms from gas-phase ethane is 712 kJ/mol. This value is calculated by taking into account the gas-phase dihydrogen dissociation energy to be 436 kJ/mol.[46] The formation of surface ethylidyne species involves breaking of three C−H bonds and the formation of three Pt−C bonds. The C−H bond energy in ethane molecule is taken to be 423 kJ/mol.[46] Hence, the Pt−C bond energy is calculated to be 186 kJ/mol. Other values reported in the Table 6 for Pt(111) and Pt(211) slabs are calculated similarly.

It can be seen in Table 6 that the average value of Pt−C bond strength is 165 kJ/mol for the Pt(111) surface. King and co-workers have reported Pt−C bond energies to be near 240 kJ/mol from their microcalorimetric studies of ethylene adsorption.[47] The difference between these values is caused by differences in the reference states for these calculations. Specifically, we calculate the electronic energy change to be 105 kJ/mol for the reaction of gas-phase ethylene to form ethylidyne species and a gas-phase hydrogen atom. We assume the C−C and C═C bond strengths to be 376 and 733 kJ/mol and C−H bond strengths in ethane and ethylene to be 423 and 465 kJ/mol, respectively.[46] The formation of ethylidyne species on platinum involves breaking of one C═C bond and two C−H bonds in ethylene and forming one C−C bond, one C−H bond as in ethane, and three Pt−C bonds. Accordingly, we then estimate that the average strength of the three Pt−C bonds formed when ethylidyne species adsorb on Pt(111) slabs is equal to 253 kJ/mol. This value is in better agreement with the value reported by King and co-workers (240 kJ/mol). Importantly, we note that the average Pt−C bond strength is higher on the Pt(211) surface than on Pt(111) surface by 29 kJ/mol.

We also report in Table 6 values of the Pt−C bond strengths calculated by a valence bond (vb) method. This method calculates the bond dissociation energy where the final state is the clean surface and gaseous species in the electronic states corresponding to those in the initial state.[48] As an example, we have calculated the Pt−C bond energy for the formation of ethylidyne species from gaseous CCH_3 with three unpaired electrons. The corresponding energy change is −683 kJ/mol, resulting in a Pt−C bond energy equal to 228 kJ/mol.

To address the nature of the bonding in the transition states, we have used the valence bond approach to estimate the Pt−C bond energies for the activated ethyl, ethylidene and vinyl species on the Pt(111) surface. For example, we calculate the energy change for the formation of activated ethyl species on the Pt(111) slab from a gaseous ethyl radical having one unpaired electron and having the same geometry as the adsorbed activated ethyl species, to be −288 kJ/mol. The C−C bond in the activated complex can be imagined to be half broken, accompanied by the formation of two new half Pt−C bonds, i.e., the formation of one new Pt−C bond. Since the stable ethyl species on Pt(111) already forms one Pt−C bond with Pt(111), we can imagine that the activated ethyl complex forms a total of two Pt−C bonds with the Pt(111) surface. Therefore, the bonding energy of −288 kJ/mol corresponds to a Pt−C bond energy of 144 kJ/mol per Pt−C bond in the activated complex. For comparison, it can be seen in Table 6 that the Pt−C bond energy for stable ethyl species is 156 kJ/mol. Similar calculations for activated ethylidene and vinyl species give total energy changes of −495 and −692 kJ/mol, respectively. These activated complexes can be imagined to form a total of 3 and 4 Pt−C bonds, respectively, with the Pt(111) surface, corresponding to Pt−C energies of 165 and 173 kJ/mol per Pt−C bond, respectively. From Table 6, it can be seen that the Pt−C bond energies for the corresponding stable species are 170 and 192, respectively. Hence, we conclude that the activated C_2H_x complexes are comprised of a half-broken C−C bond and two-half Pt−C bonds, in addition to the Pt−C bonds already existing for the stable C_2H_x(ads) species.

In addition to our estimates of the energies of the gas-phase radicals that have the same geometries as the activated complexes on the Pt (111) surface, we have also calculated the energies of the same gas-phase radicals with the C−C bond length constrained to be equal to the value in the activated complex, but allowing the hydrogen atoms to relax. This energy of relaxation is approximately equal to 100 kJ/mol for the ethyl and ethylidene species, and this value may be used as an estimate of the energy involved in bending the hydrogen atoms in the transition states from their preferred tetrahedral positions in the stable adsorbed species. In addition, we have calculated the energy changes when the C−C bond lengths in the aforementioned gaseous radicals are subsequently allowed to relax from their values near 2.00 Å in the activated species to their equilibrium values of 1.54 Å. This energy for relaxation of the C−C bond is approximately equal to 180 kJ/mol energy for the activated ethyl and ethylidene species. Therefore, we estimate that formation of the activated ethyl and ethylidene species on the Pt(111) surface involves the partial cleavage of the C−C bond (180 kJ/mol), bending of the C−H bonds (100 kJ/mol), and the formation of two, half Pt−C bonds (−160 kJ/mol). The actual values of the activation energies depend on the detailed balance of these bond-breaking/deformation and bond-forming phenomena.

Table 1 shows that the adsorbed ethylidene species has the lowest activation energy for C−C bond cleavage on Pt_{10} clusters and Pt(111). Except for the di-σ/π vinylidene species which has a partial C═C double bond, all reactant C_2H_x(ads) species of this study have a C−C bond length near 1.52 Å and Pt−C bond lengths near 2.02 Å (see Table 1). New Pt−C bonds are formed in the transition state and the C−C bond is stretched to 1.89−2.24 Å. The C−C bond length is the shortest for the activated ethylidene species. Furthermore, this activated complex makes two additional bonds with the Pt surface, which stabilizes the complex. Therefore, this activated complex has the lowest

TABLE 7: Calculated Binding Energy Differences (kJ/mol) between Pt(111) and Pt(211) for Adsorption of C_2H_x Hydrocarbon Species

species	adsorption site	energy difference
$C_2H_5^{\ddagger}$	2-fold	116
$CHCH_3$	2-fold	85
C_2H_4 (di-σ)	2-fold	71
$CHCH_2^{\ddagger}$	3-fold	48
$CHCH_2$	3-fold	47
C_2H_5	1-fold	45
$CHCH_3^{\ddagger}$	3-fold	28
CCH_3	3-fold	13

activation energy compared to other species where either new Pt−C bonds are not formed as effectively or where the C−C bond length in the activated complex is longer.

It has been shown elsewhere that trends in bond energies for adsorbates on metal surfaces can be explained in terms of the coupling of adsorbate states with the metal d electrons.[49] While the sp bands of the metal are broad and structureless, the d bands are narrow, and small changes in the environment can significantly change the d states and their interaction with adsorbate states. A simple measure of the position of the d states is the d band center, which is the center of mass relative to the Fermi energy of the density of states projected onto the atomic d states of the clean surface. For convenience, we use all the d states here, instead of the ones with the correct symmetry for bonding with various adsorbates. This approximation makes no major difference when the adsorption geometry remains similar. The calculated d band centers relative to the Fermi energy are −2.06, −2.47, and −2.49 eV for a step edge atom on Pt(211), a central terrace atom on Pt(211) and an atom on Pt(111), respectively. The coordination numbers of the step edge atom and central terrace atom on Pt(211) are 7 and 9, respectively, while that on Pt(111) is 9. The change in the d band center agrees with the general rule that lower coordination number leads to a smaller local bandwidth and higher d band center (for metals with more than half-filled d bands).

Table 7 shows the differences in binding energies on Pt(111) and Pt(211) for various adsorbates as a function of the adsorption site. We note that the strengthening effect of the higher d band center for Pt(211) depends on the type of adsorption site. The adsorbates on the 2-fold sites are strengthened more on Pt(211) compared to Pt(111), followed by the adsorbates on 1-fold and 3-fold sites. This effect may be explained simply by taking into account the number of low-coordination platinum atoms participating in the bonding. The terrace atoms of Pt(211) are like atoms on Pt(111), which is reflected in the fact that they have similar d band centers.

The calculated energy changes in Tables 2 and 3 show a significant lowering of the energies of the activated complexes on Pt(211) compared to the Pt(111). These differences are primarily caused by the lower coordination numbers of the Pt atoms participating in the bonding at the step edge. We have also investigated one mode of C−C bond cleavage for vinyl species at the special site available on the Pt(211) surface, as shown in Figures 6f and 8f. The activation energy for the elementary step to form the activated complex from the adsorbed vinyl species is calculated to be 87 kJ/mol, which is the lowest among all reaction pathways. However, the energy change to form this activated complex from gas-phase ethane with the liberation of gas-phase dihydrogen is 258 kJ/mol which is similar to the value of 241 kJ/mol for the vinyl species shown in Figure 8e. One may speculate that a longer chain molecule may be able to take better advantage of this special site available on the Pt(211) surface.

Finally, we use the results of the present paper to address the kinetics of ethane hydrogenolysis over Pt.[50] Ethane hydrogenolysis continues to be the subject of research, as investigators further refine and elucidate the interactions of hydrocarbons with metal surfaces.[7,51−53] In our previous analyses of ethane hydrogenolysis, we have shown that the dissociative adsorption of dihydrogen and the dissociative adsorption of ethane to form various C_2H_x(ads) species may be considered to be quasi-equilibrated processes. Accordingly, we may write the reaction scheme for ethane hydrogenolysis as a series of lumped equilibria involving the formation of C_2H_x(ads) species from gaseous C_2H_6 and H_2 as shown in steps 1 and 2 below.

$$H_2 + 2* \rightleftharpoons 2H* \qquad \text{(Step 1)}$$

$$C_2H_6 + * \rightleftharpoons C_2H_x* + \frac{6-x}{2}H_2 \qquad \text{(Step 2)}$$

Importantly, these lumped equilibria do not involve assumptions about the strength or mobility of adsorbed hydrogen atoms. Since the removal of each H atom from C_2H_6 to form C_2H_x(ads) involves the cleavage of a C−H bond (average strength of 423 kJ/mol[46]) with the formation of a Pt−C bond (average strength near 165 kJ/mol, see Table 6) and the formation of one-half of a H−H bond (218 kJ/mol), we may conclude that the formation of C_2H_x(ads) species becomes more endothermic (by about 40 kJ/mol) as more hydrogen atoms are removed from ethane. In addition, the standard entropy change becomes more positive as more hydrogen atoms are removed from ethane.[6] Accordingly, the formation of more highly dehydrogenated C_2H_x(ads) species is favored with increasing temperature.

According to transition state theory, the activated complex for C−C bond cleavage of a particular C_2H_x(ads) species may be assumed to be in equilibrium with that C_2H_x(ads) species. Therefore, we are able to write the formation of activated complexes for the different C−C bond cleavage steps in terms of lumped equilibria involving C_2H_x(ads) species,

$$C_2H_x* \rightleftharpoons [C_2H_x*]^{\ddagger} \longrightarrow C_1 \text{ Products} \qquad \text{(Step 3)}$$

where $[C_2H_x*]^{\ddagger}$ is the activated complex. Combination of steps 1, 2, and 3 then leads to the quasi-equilibrated formation of a particular activated complex from gas-phase ethane with the formation of gas-phase dihydrogen as shown in step 4. The rate

$$C_2H_6 + * \rightleftharpoons [C_2H_x*]^{\ddagger} + \frac{6-x}{2}H_2 \qquad \text{(Step 4)}$$

of ethane hydrogenolysis is thus controlled by the lumped equilibrium relation of step 4, which controls the surface concentration of activated complex $C_2H_x^{\ddagger}$.

Table 5 shows the enthalpy changes and Gibbs free energy changes for the formation of activated complexes, corresponding to various C−C dissociation pathways. The results from this table suggest that ethane hydrogenolysis may take place primarily through adsorbed ethyl species, while, di-σ ethylene, ethylidene, and vinyl species may also provide viable reaction pathways. Results from kinetic analyses by Sinfelt and coworkers of ethane hydrogenolysis over Pt suggested that the rate-limiting step may involve highly dehydrogenated C_2H_x(ads) species (e.g., $x = 0$).[7] More recent results of NMR investigations conducted by Klug et al. in conjunction with Sinfelt suggest that the C−C bond breaking step may involve an adsorbed

species with $x = 3$ over platinum.[54] These results for ethane hydrogenolysis illustrate the general difficulty in using analyses of reaction kinetics data alone to elucidate the nature of reaction mechanisms. This present paper illustrates how additional information about reaction mechanisms can be obtained from quantum chemical calculations that are capable of predicting structures and energetics for possible transition states.

In our previous kinetic analyses of ethane hydrogenolysis over Pt catalysts, we found that the reaction takes place by cleavage of the C−C bond in C_2H_5(ads), as well as C−C bond in a more dehydrogenated surface species such as C_2H_4(ads), C_2H_3(ads), and/or C_2H_2(ads).[50] Furthermore, the Gibbs free energy changes for the formation of these activated complexes in step 4 were found to be near 140 kJ/mol. In agreement with our previous kinetic analyses, the results in Table 5 of the present DFT study suggest that C−C bond cleavage may take place through C_2H_5(ads), with contributions also from C_2H_4(ads), C_2H_3(ads), and/or C_2H_2(ads). The value of the Gibbs free energy barrier predicted by DFT calculations for C−C cleavage of C_2H_5(ads) species on Pt(211) (164 kJ/mol) is in good agreement with the barrier estimated from kinetic analysis (140 kJ/mol), while the predicted values of the Gibbs free energy barriers for C−C cleavage of the more highly dehydrogenated C_2H_x(ads) species are higher by about 50 kJ/mol than the barriers estimated from kinetic analysis. We note, however, that the results of our DFT calculations indicate that the values of the activation barriers are strongly dependent on the geometry of the surface. Therefore, the higher values of the Gibbs free energy barriers estimated from our DFT calculations on Pt(211) seem to suggest that the active sites responsible for ethane hydrogenolysis on the Pt catalysts we studied[50] may contain Pt surface atoms with coordination numbers lower than those on the Pt(211) surface. However, we note that the errors involved in the DFT calculations and the uncertainties in the experimental barriers also contribute to the differences in the calculated and experimental values. For example, the binding energies predicted by the use of the RPBE functional[32] are lower by about 32 kJ/mol than the energies reported in this paper using the PW-91 functional for the stable species on platinum. This comparison between the energetics obtained from the two functionals may be an indicator of the uncertainty in the theoretical calculations.

It is noteworthy that the primary pathways for C−C bond cleavage may take place through activated complexes that are rather highly hydrogenated (e.g., $CHCH_3$(ads) and C_2H_5(ads)) compared to the most abundant surface intermediates (e.g., CCH_2(ads) and C_2H_3(ads)). Accordingly, the C_2H_x(ads) reactive species that are responsible for C−C bond cleavage are not necessarily the most abundant surface intermediates that can be observed spectroscopically. However, these most abundant surface intermediates still play an important role in the reaction kinetics by determining the fraction of the surface that is available for catalytic reaction (i.e., they participate in site blocking).

Conclusions

We have used cluster and slab approaches in conjunction with density functional theory to investigate the stability and reactivity of C_2H_x(ads) species on platinum. The calculated structures of C_2H_x(ads) species obtained from Pt_{10} clusters are in agreement with results obtained from Pt(111) and Pt(211) slabs. However, the slab approach is preferred to obtain energetics of the surface species, since this approach rigorously accounts for the true electronic structure and extended field effects for a well-defined surface. We show that the calculated energies of adsorption of ethylene to form di-σ-bonded ethylene and ethylidyne species on Pt(111) and adsorption of acetylene to form di-σ/π vinylidene species on Pt(211) are within 20 kJ/mol of the respective microcalorimetric values. We find that the energetics predicted by using two-layer slabs are sufficiently converged with respect to the slab thickness for periodic slab calculations (within 10 kJ/mol). Furthermore, we find that the energy changes caused by the adsorption-induced relaxations on close packed surfaces such as (111) or (211) are small (within 20 kJ/mol). Hence, we conclude that reliable energetics can be obtained by using rigid two-layer platinum slabs, which require modest computational resources. With this approach, we then obtain the energetics of surface species, which are not easily accessible to traditional experimental approaches, highly reactive intermediates and activated complexes. We have calculated the activation energies of various C−C bond dissociation steps, which are postulated to be the controlling steps in reactions such as ethane hydrogenolysis.

We have also estimated heats of adsorption at higher temperature (623 K), which facilitates comparison with experimental data. We obtain zero-point energy corrections and thermal corrections from vibrational frequencies calculated from small platinum clusters. We show that these corrections are important for reactions where several bonds are dissociated and formed. For example, at 623 K the calculated enthalpy change to form activated vinyl complex on Pt(211) surface from gas-phase ethane with the formation of gas-phase dihydrogen is lowered by 35 kJ/mol by the inclusion of the zero-point energy corrections and thermal corrections. Vibrational frequencies are also used to estimate the entropies of surface species, and these values are used to calculate the Gibbs free energy changes associated with various C−C bond dissociation steps. We show that the overall rate of C−C bond cleavage is controlled by these Gibbs free energy changes for the formation of the surface activated complexes and gaseous dihydrogen from gaseous ethane.

We show that the underlying parameter for explaining the stronger binding of various species on the step edge of Pt(211) compared to Pt(111) is the position of the metal d band center. The step edge atoms on Pt(211) surface have a narrower d-band, with the d-band center being closer to the Fermi level compared to Pt(111). The binding energy differences between these two surfaces can be large, e.g., 116 kJ/mol for the activated ethyl complex. Furthermore, we show that the average Pt−C bond energy is stronger on Pt(211) than on Pt(111) by 29 kJ/mol. Therefore, reactions involving these surface species will preferentially take place on defect sites such as the step edge of Pt(211). The large differences in the binding energies of the C_2H_x(ads) species between Pt(111) and Pt(211) are in agreement with the experimental observation that ethane hydrogenolysis is a structure sensitive reaction.

While comparison of the energetics obtained from cluster and slab approaches shows differences in predicted energetics, the predicted trends are in good agreement with each other. In addition, cluster and slab approaches give similar values for the bond lengths and angles of the adsorbed C_2H_x(ads) species, and these calculated bond lengths are in overall agreement with experimental values. This study has identified ethyl species, along with di-σ-bonded ethylene, ethylidene, and vinyl species as reactive intermediates for ethane hydrogenolysis. On the other hand, the most abundant species on Pt surface are predicted to be ethylidyne species and di-σ/π vinylidene, depending on the temperature. Thus, results from DFT calculations suggest that the most reactive intermediates may be different from the most abundant species on the Pt surface.

Acknowledgment. We acknowledge financial support for this research by the National Science Foundation. We thank Manos Mavrikakis for stimulating discussions. We thank Lars Hansen for help with the density functional total energy program.

References and Notes

(1) Norskov, J. K. *Stud. Surf. Sci. Catal.* **1999**, *122*, 3−10.
(2) Siegbahn, P. E. M. *Adv. Chem. Phys.* **1996**, *XCIII*, 333−388.
(3) van Santen, R. A.; Neurock, M. *Catal. Rev. Sci. Eng.* **1995**, *37*, 557−698.
(4) Paul, J. F.; Sautet, P. *J. Phys. Chem. B* **1998**, *102*, 1578−1585.
(5) Kua, J.; Goddard, W. A. *J. Phys. Chem. B* **1998**, *102*, 9492−9500.
(6) Watwe, R. M.; Spiewak, B. E.; Cortright, R. D.; Dumesic, J. A. *J. Catal.* **1998**, *180*, 184−193.
(7) Sinfelt, J. H. *Adv. Catal.* **1973**, *23*, 91−119.
(8) Rodriguez, J. A.; Goodman, D. W. *Surf. Sci. Rep.* **1991**, *14*, 1−107.
(9) Cassuto, A.; Kiss, J.; White, J. M. *Surf. Sci.* **1991**, *255*, 289−294.
(10) Cremer, P.; Stanners, C.; Niemantsverdriet, J. W.; Shen, Y. R.; Somorjai, G. *Surf. Sci.* **1995**, *328*, 111−118.
(11) Cremer, P. S.; Su, X.; Shen, Y. R.; Somorjai, G. A. *J. Am. Chem. Soc.* **1996**, *118*, 2942−2949.
(12) Demuth, J. E. *Surf. Sci.* **1979**, *84*, 315−328.
(13) Ibach, H.; Lehwald, S. *J. Vac. Sci. Technol.* **1979**, *15*, 407−415.
(14) Kesmodel, L. L.; Dubois, L. H.; Somorjai, G. A. *J. Chem. Phys.* **1979**, *70*, 2180−2188.
(15) Shen, J.; Hill, J. M.; Watwe, R. M.; Spiewak, B. E.; Dumesic, J. A. *J. Phys. Chem. B* **1999**, *103*, 3923−3934.
(16) Sheppard, N. *Annu. Rev. Phys. Chem.* **1988**, *39*, 589−644.
(17) Sheppard, N.; de la Cruz, C. *Adv. Catal.* **1996**, *41*, 1.
(18) Stuck, A.; Wartnaby, C. E.; Yeo, Y. Y.; King, D. A. *Phys. Rev. Lett.* **1995**, *74*, 578−581.
(19) Yeo, Y. Y.; Stuck, A.; Wartnaby, C. E.; King, D. A. *Chem. Phys. Lett.* **1996**, *259*, 28−36.
(20) Yeo, Y. Y.; Wartnaby, C. E.; King, D. A. *Science* **1995**, *268*, 1731−1732.
(21) Natal-Santiago, N. A.; Podkolzin, S. G.; Cortright, R. D.; Dumesic, J. A. *Catal. Lett.* **1997**, *45*, 155.
(22) Cortright, R. D.; Dumesic, J. A. *J. Catal.* **1994**, *148*, 771−778.
(23) Spiewak, B. E.; Cortright, R. D.; Dumesic, J. A. *J. Catal.* **1998**, *176*, 405−414.
(24) *Jaguar*, 3.5 ed.; Schrodinger, Inc.: Portland, OR, 1998.
(25) Becke, A. D. *J. Chem. Phys.* **1993**, *98*, 5648.
(26) Hay, P. J.; Wadt, W. R. *J. Chem. Phys.* **1985**, *82*, 299−310.
(27) Hehre, W. J.; Radom, L.; Schleyer, P. v. R.; Pople, J. A. *Ab initio Molecular Orbital Theory*; John Wiley: New York, 1987.
(28) Vanderbilt, D. H. *Phys. Rev. B* **1990**, *41*, 7892.
(29) White, J. A.; Bird, D. M. *Phys. Rev. B* **1994**, *50*, 4954.
(30) Perdew, J. P.; Chevary, J. A.; Vosko, S. H.; Jackson, K. A.; Pederson, M. R.; Singh, D. J.; Fiolhais, C. *Phys. Rev. B* **1992**, *46*, 6671.
(31) Kresse, G.; Furthmuller, J. *Comput. Mater. Sci.* **1996**, *6*, 15.
(32) Hammer, B.; Hansen, L. B.; Nørskov, J. K. *Phys. Rev. B* **1999**, *59*, 7413.
(33) Somorjai, G. A. *Introduction to Surface Chemistry and Catalysis*; John Wiley and Sons: New York, 1994.
(34) Sharma, S. B.; Miller, J. T.; Dumesic, J. A. *J. Catal.* **1994**, *148*, 198.
(35) Christmann, K. *Surf. Sci. Rep.* **1988**, *9*, 1−163.
(36) Paul, J. F.; Sautet, P. *J. Phys. Chem.* **1994**, *98*, 10906−10912.
(37) Kang, D.; Anderson, A. *Surf. Sci.* **1985**, *155*, 639−652.
(38) Maurice, V.; Minot, C. *Langmuir* **1989**, *5*, 734−741.
(39) Ge, Q.; King, D. A. *J. Chem. Phys.* **1999**, *110*, 4699−4702.
(40) Döll, R.; Gerken, C. A.; Van Hove, M. A.; Somorjai, G. A. *Surf. Sci.* **1997**, *374*, 151−161.
(41) Stohr, J.; Gland, J. L.; Horsley, J. A. *Chem. Phys. Lett.* **1984**, *105*, 332.
(42) Stohr, J.; Sette, F.; Johnson, A. L. *Phys. Rev. Lett.* **1984**, *53*, 1684.
(43) Starke, U.; Barbieri, A.; Materer, N.; Van Hove, M. A.; Somorjai, G. A. *Surf. Sci.* **1993**, *286*, 1−14.
(44) Wang, P.-K.; Slichter, C. P.; Sinfelt, J. H. *Phys. Rev. Lett.* **1984**, *53*, 82−85.
(45) Kose, R.; Brown, W. A.; King, D. A. *J. Am. Chem. Soc.* **1999**, *121*, 4845−4851.
(46) *CRC Handbook of Chemistry and Physics*, 79th ed.; Lide, D. R., Ed.; CRC Press: Boca Raton, 1998−1999.
(47) Brown, W. A.; Kose, R.; King, D. A. *Chem. Rev.* **1998**, *98*, 797−831.
(48) Carter, E. A.; Koel, B. E. *Surf. Sci.* **1990**, *226*, 339−357.
(49) Hammer, B.; Norskov, J. K. *Theory of Adsorption and Surface Reactions*; NATO ASI Series E: Applied Sciences, Chemisorption and Reactivity on Supported Clusters and Thin Films; Erice, Trapani: Sicily, 1996.
(50) Cortright, R. D.; Watwe, R. M.; Spiewak, B. E.; Dumesic, J. A. *Catal. Today* **1999**, *53*, 395−406.
(51) Larsson, R. *Catal. Lett.* **1992**, *13*, 71−86.
(52) Shang, S. B.; Kenney, C. N. *J. Catal.* **1992**, *134*, 134−150.
(53) Bond, G. C.; Cunningham, R. H. *J. Catal.* **1997**, *166*, 172−185.
(54) Klug, C. A.; Slichter, C. P.; Sinfelt, J. H. *Isr. J. Chem.* **1992**, *32*, 185.